Chemical Science

ROYAL SOCIETY OF CHEMISTRY

EDGE ARTICLE

View Article Online
View Journal | View Issue

Cite this: *Chem. Sci.*, 2021, **12**, 7937

All publication charges for this article have been paid for by the Royal Society of Chemistry

Received 19th March 2021
Accepted 4th May 2021

DOI: 10.1039/d1sc01580j

rsc.li/chemical-science

Reactivity of cyano- and isothiocyanatoborylenes: metal coordination, one-electron oxidation and boron-centred Brønsted basicity†

Stephan Hagspiel,[ab] Dren Elezi,[ab] Merle Arrowsmith,[ab] Felipe Fantuzzi,[ab] Alfredo Vargas,[c] Anna Rempel,[ab] Marcel Härterich,[ab] Ivo Krummenacher[ab] and Holger Braunschweig *[ab]

Doubly base-stabilised cyano- and isothiocyanatoborylenes of the form LL′BY (L = CAAC = cyclic alkyl(amino)carbene; L′ = NHC = N-heterocyclic carbene; Y = CN, NCS) coordinate to group 6 carbonyl complexes *via* the terminal donor of the pseudohalide substituent and undergo facile and fully reversible one-electron oxidation to the corresponding boryl radical cations $[LL'BY]^{\bullet+}$. Furthermore, calculations show that the borylenes have very similar proton affinities, both to each other and to NHC superbases. However, while the protonation of LL′B(CN) with PhSH yielding $[LL'BH(CN)^+][PhS^-]$ is fully reversible, that of LL′B(NCS) is rendered irreversible by a subsequent B-to-C_{CAAC} hydrogen shift and nucleophilic attack of PhS^- at boron.

Introduction

With their lone pair at boron and two empty p orbitals monocoordinate borylenes (:BY, Y = anionic substituent), with boron in its +1 oxidation state, have only been observed spectroscopically by microwave and near-ultraviolet spectroscopy[1] or in inert gas matrices at extremely low temperatures,[2] and their transient generation has long been postulated by various trapping reactions.[1–3] While at first the isolation of borylenes under ambient conditions was only achieved in the coordination sphere of electron-rich transition metals,[4] the last decade has seen the emergence of metal-free borylenes stabilised by strong donor–acceptor ligands.[5] The first metal-free borylene, designed by Bertrand and co-workers in 2011 (**I**, Fig. 1),[6] owed its stability to the two cyclic (alkyl)(amino)carbene (CAAC) ligands,[7] which stabilise the empty p orbitals of the borylene through σ donation and the lone pair at boron through π backdonation to the π-acidic carbene centres. Since then CAAC ligands have been successfully employed to access the first stable dicoordinate aminoborylene,[8] as well as a wide range of tricoordinate borylenes of the form (CAAC)LBY, where L is a neutral donor ligand (*e.g.* N-heterocyclic carbene (NHC), phosphine, CO, N_2, *etc.*) and Y is an anionic substituent (*e.g.* aryl,[9] amino,[8] boryl,[10] H,[10a,11] F,[12] Cl,[13] CN,[14] NCS,[15] *etc.*).

While much less reactive than mono- or dicoordinate borylenes, tricoordinate borylenes display typical boron-centred borylene reactivity, including, but not limited to, boron coordination to Lewis acids and transition metals, one-electron oxidation and Brønsted basicity.

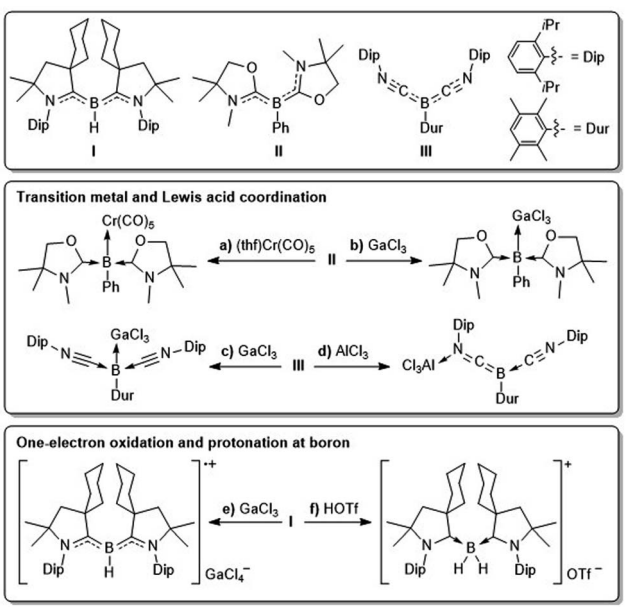

Fig. 1 Selected examples of reactivity of tricoordinate borylenes.

[a]*Institute for Inorganic Chemistry, Julius-Maximilians-Universität Würzburg, Am Hubland, 97074 Würzburg, Germany. E-mail: h.braunschweig@uni-wuerzburg.de*

[b]*Institute for Sustainable Chemistry & Catalysis with Boron, Julius-Maximilians-Universität Würzburg, Am Hubland, 97074 Würzburg, Germany*

[c]*Department of Chemistry, School of Life Sciences, University of Sussex, Brighton BN1 9QJ, Sussex, UK*

† Electronic supplementary information (ESI) available: Synthetic procedures, NMR, IR, UV-vis, CV, EPR and details of the computational analyses. CCDC 2071470–2071477. For ESI and crystallographic data in CIF or other electronic format see DOI: 10.1039/d1sc01580j

Kinjo showed, for example, that bis(oxazol-2-ylidene)-stabilised phenylborylene **II** can coordinate as a neutral σ donor to chromium(0) and group 9 precursors, as well as $GaCl_3$ (Fig. 1a,b).[16] Similarly, our group has reported Lewis adduct formation between the bis(isonitrile)-stabilised arylborylene **III** and $GaCl_3$ (Fig. 1c), whereas the hard Lewis acid $AlCl_3$ coordinates at the isonitrile nitrogen (Fig. 1d).[17] Furthermore, borylene **I** undergoes facile one-electron oxidation to the corresponding boryl radical cation,[6] in which boron adopts a formal +2 oxidation state and spin density is mainly delocalised over the B–C_{CAAC} π bonds (Fig. 1e). Finally, while dicoordinate neutral and cationic borylenes are known to activate H_2,[8,18] and transient dicoordinate borylenes have been observed to insert into intramolecular C–H and C–C σ bonds,[3b,19] examples of σ bond activation by tricoordinate borylenes remain limited to the protonation at boron by strong Brønsted acids. Thus borylenes **I** and **II** can be protonated with triflic acid, generating the corresponding hydroboronium triflates (Fig. 1f).[6,16b]

In this study, we explore the reactivity of tricoordinate pseudohaloborylenes of the form (CAAC)(NHC)BY (Y = CN, NCS), as neutral donors to group 6 transition metals, in one-electron oxidation reactions, and as boron-centred Brønsted bases in reversible and irreversible protonations with thiophenol.

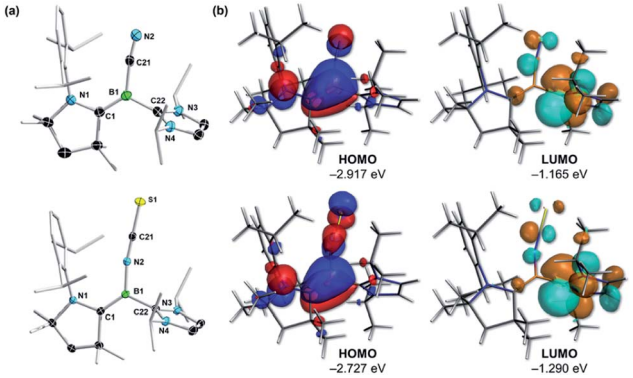

Fig. 2 (a) Crystallographically-derived molecular structures of (*Z*)-2^{CN} and (*Z*)-2^{NCS} (only one of the two molecules of (*Z*)-2^{CN} and (*Z*)-2^{NCS} present in the asymmetric unit is represented). Thermal ellipsoids drawn at the 50% probability level. Ellipsoids on the CAAC ligand periphery and hydrogen atoms omitted for clarity. Selected bond lengths (Å) for (*Z*)-2^{CN}: N1–C1 1.4076(14), C1–B1 1.4630(17), B1–C21 1.5490(18), C21–N2 1.1618(16), B1–C22 1.5918(16). For (*Z*)-2^{NCS}: N1–C1 1.4080(14), C1–B1 1.4591(16), B1–N2 1.4836(15), N2–C21 1.1706(15), C21–S1 1.6195(12). (b) Canonical Kohn–Sham molecular orbitals of (*Z*)-2^{CN} (top) and (*Z*)-2^{NCS} (bottom) at the OLYP/TZ2P level of theory. Selected Hirshfeld atomic charges for (*Z*)-2^{CN}: N1: −0.055; C1: −0.050; B1: −0.064; C21: −0.032; N2: −0.282; C22: +0.076; for (*Z*)-2^{NCS}: N1: −0.061; C1: −0.068; B1: −0.012; N2: −0.142; C21: +0.035; S1: −0.210; C22: +0.072.

Results and discussion

Synthesis of tricoordinate pseudohaloborylenes

The tricoordinate cyanoborylene (CAAC)(I^iPr)B(CN) (2^{CN}, CAAC = 1-(2,6-diisopropylphenyl)-3,3,5,5-tetramethylpyrrolidin-2-ylidene; I^iPr = 1,3-diisopropylimidazol-2-ylidene) and isothiocyanatoborylene (CAAC)(I^iPr)B(NCS) (2^{NCS})[15] were synthesised by the reduction of the corresponding dibromoborane precursors, (CAAC)BBr_2(CN) (1^{CN})[14] and (CAAC)BBr_2(NCS) (1^{NCS}),[15] respectively, with 2.2 equiv. KC_8 in benzene in the presence of 2.2 equiv. I^iPr (Scheme 1).

The cyanoborylene 2^{CN} was isolated as a yellow crystalline solid and showed an ^{11}B NMR resonance at −12.1 ppm, similar to the related cyanoborylene (CAAC)(IMe)B(CN) (δ_{11B} = −11.3 ppm; IMe = 1,3,4,5-tetramethylimidazol-2-ylidene).[14] This contrasts with 2^{NCS}, which is formed as a 22 : 78 mixture of the (*E*)- and (*Z*)-isomer with regards to the arrangement of the NCS unit and CAAC nitrogen atom across the B=C_{CAAC} double bond, each isomer showing a distinct ^{11}B NMR resonance ((*E*)-2^{NCS}: δ_{11B} = 3.8 ppm; (*Z*)-2^{NCS}: δ_{11B} = −2.6 ppm).[15] The solid-state structure of 2^{CN} (Fig. 2a) shows the *Z*-isomer. Both (*Z*)-2^{CN} and (*Z*)-2^{NCS} display structural parameters typical for CAAC–NHC–stabilised tricoordinate borylenes,[9–11,13,14] with trigonal planar boron centres and short B–C_{CAAC} bonds (*ca.* 1.45 Å) with double bond character, indicating strong π backbonding from the borylene centre to the π-acidic CAAC ligand. In both compounds the NHC rings are rotated almost perpendicularly to the borylene plane (torsion angle C1–B1–C22–N3 *ca.* 85–98°) and coordinating as pure σ donors (B1–C22 *ca.* 1.59 Å).

Accordingly, their HOMOs are composed of strong π contributions in the B–C_{CAAC} bonding region, with negligible involvement of the C_{NHC} atom, while their LUMOs feature the vacant C_{NHC} p orbitals (Fig. 2b). The more negative Hirshfeld charge at boron for (*Z*)-2^{CN} (−0.064) than for (*Z*)-2^{NCS} (−0.012) indicates that the former is more electron-rich than the latter, in agreement with the relative ^{11}B NMR shifts of the two compounds.

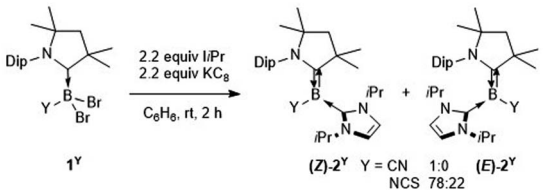

Scheme 1 Synthesis of cyano- and isothiocyanatoborylenes 2^{CN} and 2^{NCS}.

Coordination to group 6 transition metal carbonyls

The addition of (*Z*)-2^{CN} or (*Z*)-2^{NCS} to irradiated THF solutions of group 6 carbonyl precursors, [M(CO)$_6$] (M = Cr, Mo, W), resulted in an instant intensification of the solution colour. After removal of the solvent, complexes 2^{CN}-**M** (M = Cr, Mo, W) and 2^{NCS}-**M** (M = Cr, W) were isolated as yellow-brown and red-brown solids, respectively (Scheme 2).‡ The ^{11}B NMR resonances of these compounds were only shifted *ca.* 1 ppm upfield from those of the corresponding borylene precursors (2^{CN}-**M**: δ_{11B} = −13.2 to −13.8 ppm; 2^{NCS}-**M**: δ_{11B} = −3.8 to −3.9 ppm), thus indicating that the boron centres remain tricoordinate. Significant shifts in the ^1H NMR resonances of the CAAC and

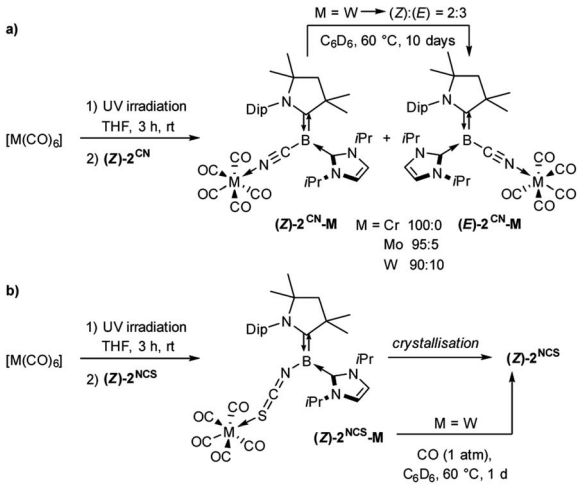

Scheme 2 Adduct formation between (Z)-2^{Y} and group 6 hexacarbonyls.

I^{i}Pr ligands, however, suggested the formation of adducts by metal coordination to the terminal nitrogen and sulphur donors of $\mathbf{2^{CN}}$ and $\mathbf{2^{NCS}}$, respectively (see Fig. S30 in the ESI†). The solid-state IR spectra of $\mathbf{2^{CN}}$-**M** and $\mathbf{2^{NCS}}$-**M** each showed four CO stretching bands in the 1850–2070 cm^{-1} and 1880–2060 cm^{-1} regions, respectively, confirming that one CO ligand had indeed been replaced. While the ^{11}B NMR spectrum of $\mathbf{2^{CN}}$-**Cr** showed only the (Z)-isomer, $\mathbf{2^{CN}}$-**Mo** and $\mathbf{2^{CN}}$-**W** were formed as a mixture of the (Z)- and (E)-isomers in a 95 : 5 and 90 : 10 ratio, respectively. Furthermore, while $(\mathbf{Z})$-$\mathbf{2^{CN}}$-**Cr** and $(\mathbf{Z})$-$\mathbf{2^{CN}}$-**Mo** did not isomerise at higher temperatures, prolonged heating of a C_6D_6 solution of the isolated 90 : 10 $(Z)/(E)$ mixture of $\mathbf{2^{CN}}$-**W** at 60 °C afforded a 2 : 3 $(Z)/(E)$ mixture, showing that the (Z)-isomer is the kinetic and the (E)-isomer the thermodynamic product (see Fig. S31 and S32 in the ESI†).§

X-ray crystallographic analyses of $\mathbf{2^{CN}}$-**M** (Fig. 3) confirmed that adduct formation occurred through the cyano nitrogen atom rather than the electron-rich boron centre, and furthermore confirmed the configuration of the B=C$_{CAAC}$ bonds in $(\mathbf{Z})$-$\mathbf{2^{CN}}$-**Cr**, $(\mathbf{Z})$-$\mathbf{2^{CN}}$-**Mo** and $(\mathbf{E})$-$\mathbf{2^{CN}}$-**W** (Fig. 2a). The bond lengths and angles in the borylene moiety of these complexes do not differ significantly from those in $(\mathbf{Z})$-$\mathbf{2^{CN}}$. The N2–M bond lengths (N2–Cr 2.0614(17), N2–Mo 2.200(3), N2–W 2.163(3) Å) are typical for nitrile–carbonyl complexes of the chromium triade.[20] Although $\mathbf{2^{NCS}}$-**M** could be isolated as powders by removal of the reaction solvent *in vacuo*, all attempts to obtain single crystals of $\mathbf{2^{NCS}}$-**M** resulted in quantitative recovery of the starting borylene $(\mathbf{Z})$-$\mathbf{2^{NCS}}$, indicating a very weak S→M interaction. Similarly, heating a C_6D_6 solution of $\mathbf{2^{NCS}}$-**W** under a CO atmosphere led to full recovery of $(\mathbf{Z})$-$\mathbf{2^{NCS}}$ and [W(CO)$_6$] within one day. A literature search showed that there have been no other reports of group 6 M^0 complexes with RN=C=S donor ligands. At first sight the preferred coordination of M(CO)$_5$ at the pendant CN and NCS ligands of $\mathbf{2^{CN}}$ and $\mathbf{2^{NCS}}$, respectively, rather than at the borylene centres, seems mostly due to the excessive steric congestion of the latter by the CAAC and I^{i}Pr ligands. Indeed, a comparison with the ^{11}B NMR shift of borylene **II** ($\delta_{11B} = -1.1$ ppm, Fig. 1), which coordinates to transition metals as a borylene donor,[16] suggests that the borylene centre in $(\mathbf{Z})$-$\mathbf{2^{NCS}}$ ($\delta_{11B} = -2.6$ ppm) should be similarly nucleophilic to **II**, while that of $(\mathbf{Z})$-$\mathbf{2^{CN}}$ ($\delta_{11B} = -12.1$ ppm) should be even more nucleophilic. However, the calculated Hirshfeld charges of the terminal CN nitrogen (−0.282) and NCS sulphur atoms (−0.210) in $(\mathbf{Z})$-$\mathbf{2^{CN}}$ and $(\mathbf{Z})$-$\mathbf{2^{NCS}}$, respectively, are significantly more negative than those of the boron atoms ($(\mathbf{Z})$-$\mathbf{2^{CN}}$: −0.064; $(\mathbf{Z})$-$\mathbf{2^{NCS}}$: −0.012, see legend of Fig. 2b), which further favours coordination at the CN and NCS ligands.

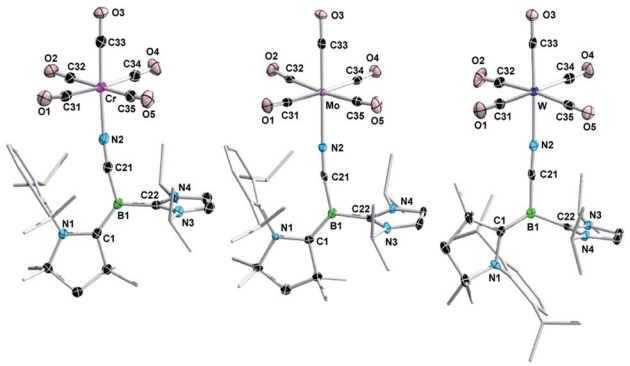

Fig. 3 Crystallographically-derived molecular structures of $(\mathbf{Z})$-$\mathbf{2^{CN}}$-**Cr**, $(\mathbf{Z})$-$\mathbf{2^{CN}}$-**Mo** and $(\mathbf{E})$-$\mathbf{2^{CN}}$-**W** (from left to right). Thermal ellipsoids drawn at 50% probability level. Ellipsoids on the CAAC ligand periphery and hydrogen atoms omitted for clarity. Selected bond lengths (Å) for $(\mathbf{Z})$-$\mathbf{2^{CN}}$-**Cr**: N1–C1 1.399(2), C1–B1 1.456(3), B1–C21 1.542(3), C21–N2 1.158(2), B1–C22 1.588(3), N2–Cr 2.0614(17), Cr–C33 1.842(2), C33–O3 1.154(2). For $(\mathbf{Z})$-$\mathbf{2^{CN}}$-**Mo**: N1–C1 1.382(5), C1–B1 1.468(5), B1–C21 1.544(5), C21–N2 1.157(4), B1–C22 1.573(6), N2–Mo 2.200(3), Mo–C33 1.961(3), C33–O3 1.166(4). For $(\mathbf{E})$-$\mathbf{2^{CN}}$-**W**: N1–C1 1.408(5), C1–B1 1.436(6), B1–C21 1.541(6), C21–N2 1.156(5), B1–C22 1.596(5), N2–W 2.163(3), W–C33 1.978(4), C33–O3 1.154(5).

One-electron oxidation

The cyclovoltammograms of $(\mathbf{Z})$-$\mathbf{2^{Y}}$ in THF showed a fully reversible redox event at $E_{1/2} = -1.06$ V (Y = NCS) and a partially reversible redox event at $E_{1/2} = -0.89$ V (Y = CN), respectively (*vs.* the ferrocene standard Fc/Fc^{+}), suggesting the possibility of selective chemical one-electron oxidation (see Fig. S51 and S52 in the ESI†). Indeed, the room temperature reactions of $(\mathbf{Z})$-$\mathbf{2^{Y}}$ with exactly one equivalent of silver triflate (AgOTf) in benzene

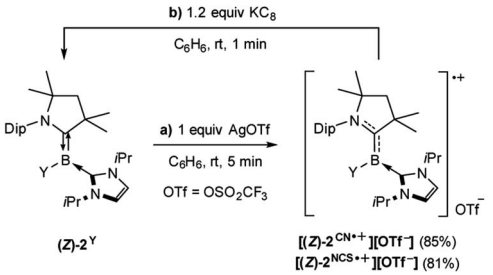

Scheme 3 Reversible chemical one-electron oxidation of $(\mathbf{Z})$-$\mathbf{2^{Y}}$ to [$(\mathbf{Z})$-$\mathbf{2^{Y\bullet+}}$][OTf^{-}], Y = CN, NCS.

resulted in a colour change from red to yellow (Y = NCS) or intensification of the yellow colour (Y = CN), respectively, accompanied by the formation of a black silver precipitate. After workup, the boryl radical cations [(*Z*)-$2^{Y\bullet+}$][OTf^-] were isolated as yellow crystals in 81% (Y = NCS) and 85% (Y = CN) yield (Scheme 3a). Conversely, the reduction of isolated [(*Z*)-$2^{Y\bullet+}$][OTf^-] with KC_8 in benzene afforded borylenes (*Z*)-2^Y in quantitative yield (Scheme 3b). The EPR spectrum of [(*Z*)-$2^{NCS\bullet+}$][OTf^-] (Fig. 4) showed a broad resonance at g_{iso} = 2.003. In contrast, that of [(*Z*)-$2^{CN\bullet+}$][OTf^-] displayed a multiplet at g_{iso} = 2.0025 with hyperfine coupling parameters to the boron ($a^{10,11B}$ = 9.0 MHz), as well as the CAAC- and cyano-nitrogen nuclei (a^{14N} = 21.7, 18.0 MHz). X-ray crystallographic analyses confirmed that the boryl radical cations [(*Z*)-$2^{Y\bullet+}$][OTf^-] retain the (*Z*)-configuration of the starting borylenes (Fig. 4). The boron centres remain trigonal planar ($\sum(\angle B) = 360°$), with a slight elongation of the C1–B1 bonds to a partial B–C double bond (*ca.* 1.51 Å), concomitant with shortening of the N1–C1 (*ca.* 1.34 Å) bonds, as expected upon one-electron oxidation of CAAC-stabilised borylenes.[6,12] Calculations show that the spin density in both radical cations is delocalised over the [(N–C)$_{CAAC}$–B–Y] π framework (Fig. 4), with the highest contribution at boron (0.388 for Y = CN; 0.295 for Y = NCS). The lower spin density at boron compared to Bertrand's CAAC-stabilized hydroboryl radical cations (0.50)[6,11] is owed to the additional delocalization of the spin density over the CN and NCS fragments, respectively.

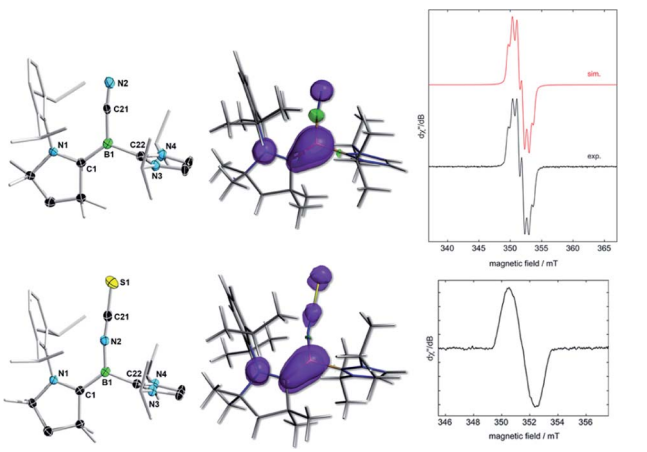

Fig. 4 Left: crystallographically-derived molecular structures of [(*Z*)-$2^{CN\bullet+}$][OTf^-] (top) and [(*Z*)-$2^{NCS\bullet+}$][OTf^-] (bottom). Thermal ellipsoids drawn at the 50% probability level. Triflate anion, ellipsoids on the CAAC ligand periphery and hydrogen atoms omitted for clarity. Selected bond lengths (Å) for [(*Z*)-$2^{CN\bullet+}$][OTf^-]: N1–C1 1.335(6), C1–B1 1.510(7), B1–C21 1.548(7), C21–N2 1.146(6), B1–C22 1.590(7); for [(*Z*)-$2^{NCS\bullet+}$][OTf^-]: N1–C1 1.342(2), C1–B1 1.510(2), B1–N2 1.454(2), N2–C21 1.170(2), C21–S1 1.5835(18), B1–C22 1.590(2). Centre: plots of spin density of [(*Z*)-$2^{CN\bullet+}$] (top) and [(*Z*)-$2^{NCS\bullet+}$] (bottom) obtained from the multipole-derived charges up to quadruple expansion (MDC-q) at the OLYP/TZ2P level of theory. Selected spin densities for [(*Z*)-$2^{CN\bullet+}$]: N1: 0.219; C1: 0.125; B1: 0.388; C21: −0.009; N2: 0.134; for [(*Z*)-$2^{NCS\bullet+}$]: N1: 0.220; C1: 0.179; B1: 0.295; N2: 0.013; C21: 0.058; S1: 0.103. Right: Experimental (black line) and simulated (red line) continuous-wave X-band EPR spectra of [(*Z*)-$2^{CN\bullet+}$][OTf^-] (top) and [(*Z*)-$2^{NCS\bullet+}$][OTf^-] (bottom) in benzene at room temperature. Best-fit simulation parameters for [(*Z*)-$2^{CN\bullet+}$]: g_{iso} = 2.0025, $a(^{10,11}B)$ = 9.0 MHz, $a(^{14}N)$ = 21.7 MHz, and $a(^{14}N)$ = 18.0 MHz.

Boron-centred Brønsted basicity

Given that tricoordinate borylenes can be protonated by the strong Brønsted acid HOTf ($pKa_{(DMSO)} = -14.3$),[6,16b,21] we sought to determine the relative Brønsted basicity of $\mathbf{2^{CN}}$ and $\mathbf{2^{NCS}}$ using the much weaker acid thiophenol ($pK_{a(DMSO)}$ = 10.3).[22] The reaction of (*Z*)-$\mathbf{2^{NCS}}$ with 1.2 equiv. PhSH at room temperature in benzene resulted in a 3 : 2 mixture of the thiolatoborane $\mathbf{3^{NCS}}$ (δ_{11B} = −6.0 ppm) and the hydroboronium species [$\mathbf{2^{NCS}}$-H+][$\mathbf{PhS^-}$] (δ_{11B} = −18.9 ppm). The $^1H\{^{11}B\}$ NMR spectrum of the product mixture showed a broad B*H* resonance at 3.76 ppm for [$\mathbf{2^{NCS}}$-$\mathbf{H^+}$] and a ^1H singlet at 3.70 ppm for $\mathbf{3^{NCS}}$, characteristic of a C1-protonated CAAC ligand.[23] Over the course of three days at room temperature in solution [$\mathbf{2^{NCS}}$-H+][$\mathbf{PhS^-}$] converted entirely to $\mathbf{3^{NCS}}$, which was identified by X-ray crystallographic analysis as the product of the formal 1,2-addition of the S–H bond to the B=C_{CAAC} double bond (Scheme 4b, Fig. S33–S36†). The conversion of [$\mathbf{2^{NCS}}$-H+][$\mathbf{PhS^-}$] to $\mathbf{3^{NCS}}$ proceeds *via* a B-to-C_{CAAC} hydride shift typical for CAAC-stabilised hydroboranes and hydroboronium species,[23] followed by nucleophilic attack of the PhS^- anion at the three-coordinate cationic boron centre. Both the reactions of [$\mathbf{2^{NCS}}$-H+][$\mathbf{PhS^-}$] and (*Z*)-$\mathbf{2^{NCS}}$ with an excess of thiophenol at 60 °C cleanly yielded the tricoordinate dithiolatoborane **4** (δ_{11B} = 42.6 ppm), alongside the imidazolium salt ([I^iPr-H][NCS]) as a by-product (Scheme 4d and e).

In contrast, the analogous reaction of (*Z*)-$\mathbf{2^{CN}}$ with 1.2 equiv. PhSH proceeded cleanly to the hydroboronium species [$\mathbf{2^{CN}}$-$\mathbf{H^+}$] (δ_{11B} = −30.3 ppm), which was identified by X-ray diffraction analysis (Scheme 4a). To our surprise, however, isolated crystals

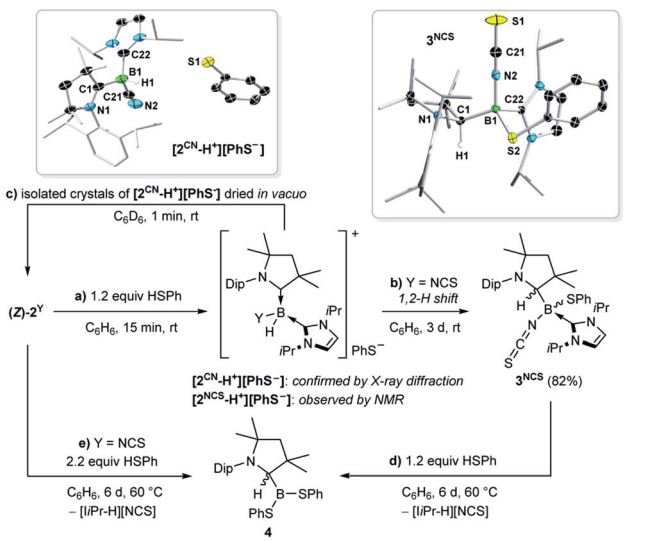

Scheme 4 Reversible and irreversible protonation of (*Z*)-$\mathbf{2^{CN}}$ and (*Z*)-$\mathbf{2^{NCS}}$, respectively, with PhSH, and crystallographically-derived molecular structures of [$\mathbf{2^{CN}}$-$\mathbf{H^+}$][$\mathbf{PhS^-}$] and $\mathbf{3^{NCS}}$. Thermal ellipsoids drawn at 50% probability level. Ellipsoids on the CAAC ligand periphery and hydrogen atoms omitted for clarity, except for the boron-bound hydride in [$\mathbf{2^{CN}}$-$\mathbf{H^+}$] and C1-bound proton in $\mathbf{3^{NCS}}$.

of $[\mathbf{2^{CN}}\text{-}\mathbf{H^+}][\mathbf{PhS^-}]$ dried *in vacuo* and redissolved in C_6D_6 yielded a yellow solution, the NMR data of which matched (*Z*)-$\mathbf{2^{CN}}$ (Scheme 4c). Moreover, isolated crystals of $[\mathbf{2^{CN}}\text{-}\mathbf{H^+}][\mathbf{PhS^-}]$ washed with hexane, left to dry in the glovebox at atmospheric pressure for one hour and redissolved in C_6D_6 yielded a solution of $\mathbf{2^{CN}}$ with only a small amount of residual PhSH, the rest having evaporated (see Fig. S37–S40†). While heating a suspension of $[\mathbf{2^{CN}}\text{-}\mathbf{H^+}][\mathbf{PhS^-}]$ in d_8-toluene showed that the concentration of $\mathbf{2^{CN}}$ and PhSH in solution increased steadily from 25 to 100 °C, the lack of solubility of the boronium salt in suitable NMR solvents prevented a quantitative analysis of the acid–base equilibrium.

Given the above-mentioned difficulties in assessing the relative Brønsted basicity of $\mathbf{2^{CN}}$ and $\mathbf{2^{NCS}}$ experimentally, gas-phase proton affinity (PA) calculations were performed (see ESI† for details). The calculated gas-phase PA for PhS^- (339.4 kcal mol^{-1}) is in good agreement with the experimental value of 349.0 ± 2 kcal mol^{-1}.[24] The PAs calculated for $\mathbf{2^{CN}}$ and $\mathbf{2^{NCS}}$, 267.9 and 268.3 kcal mol^{-1}, respectively, are identical within the error of the calculation. While at first sight these results seem in contradiction with the experimental observations of reversible protonation for $\mathbf{2^{CN}}$ and irreversible protonation for $\mathbf{2^{NCS}}$, the latter is only rendered irreversible by the subsequent B-to-C hydrogen shift and nucleophilic attack of PhS^- at boron. The higher PA of PhS^- confirms that the thiolate is more basic than $\mathbf{2^{CN}}$ and $\mathbf{2^{NCS}}$, as suggested by the reversibility of the protonation of $\mathbf{2^{CN}}$ by PhSH. Furthermore, the PAs of $\mathbf{2^{CN}}$ and $\mathbf{2^{NCS}}$ are comparable to those of the superbases CsOH (267 kcal mol^{-1})[25] and the unsaturated NHCs, 1,3-dialkyl/diarylimidazol-2-ylidenes (262–275 kcal mol^{-1}).[26]

Conclusions

We have shown that cyano- and isothiocyanatoborylenes of the form (CAAC)(NHC)BY (Y = CN $\mathbf{2^{CN}}$, NCS $\mathbf{2^{NCS}}$) are easily synthesised by the twofold reduction of (CAAC)BBr_2Y in the presence of the NHC ligand. Computational analyses show that the HOMO of these borylenes is delocalised over the entire [(N–C)$_{CAAC}$–B–Y] π framework, with a major π-bonding contribution at the B–C_{CAAC} bond. While the borylene centre bears a slightly negative partial charge the main negative charge is located at the terminal CN nitrogen and NCS sulphur atoms, respectively. As a consequence, these compounds act as neutral nitrogen-/sulphur-centred rather than boron-centred donors towards group 6 carbonyls, generating the corresponding CN→M and NCS→M adducts, respectively, under photolytic conditions. The electron-rich borylene centre of $\mathbf{2^{Y}}$, however, can undergo reversible electrochemical and chemical one-electron oxidation to the corresponding $[\mathbf{2^{Y\cdot+}}]$ radical cation. The spin density of the latter is delocalised over the [(N–C)$_{CAAC}$–B–Y] π framework, with a relatively large spin density at boron (0.388 for Y = CN; 0.295 for Y = NCS). Finally, both borylenes act as boron-centred Brønsted bases toward relatively weakly acidic thiophenol ($pK_{a(DMSO)}$ = 10.3). Whereas the protonation of $\mathbf{2^{NCS}}$ at boron is driven by a B-to-C_{CAAC} hydride shift and irreversible nucleophilic attack of PhS^- at boron, the protonation of $\mathbf{2^{CN}}$ to the corresponding boronium species is fully reversible. Calculations show that $\mathbf{2^{CN}}$ and $\mathbf{2^{NCS}}$ have in fact similar proton affinities (*ca.* 268 kcal mol^{-1}), of the same order as the inorganic superbase CsOH or unsaturated NHCs. The unprecedented reversibility of the protonation for $\mathbf{2^{CN}}$ is of particular interest as reversible small molecule activation is promising for potential catalytic applications of these species.

Author contributions

H. B. supervised the study. S. H. and D. E. carried out the synthetic work. I. K. carried out and analysed the EPR and CV experiments. S. H., A. R. and M. H. carried out the X-ray crystallographic analyses. F. F. and A. V. carried out the computational studies. M. A., S. H. and F. F. prepared the manuscript and the ESI. All authors read and commented on the manuscript.

Conflicts of interest

The authors declare no conflict of interest.

Acknowledgements

The authors thank the Deutsche Forschungsgemeinschaft for financial support. S. H. is grateful for a doctoral fellowship from the Studienstiftung des deutschen Volkes. F. F. thanks the Coordenação de Aperfeiçoamento de Pessoal de Nível Superior (CAPES) and the Alexander von Humboldt (AvH) Foundation for a Capes-Humboldt postdoctoral fellowship. A. V. thanks the University of Sussex for financial support.

Notes and references

‡ All attempts to synthesise the analogous complex $\mathbf{2^{NCS}}$-**Mo** only led to intractable mixtures of unidentifiable compounds.

§ Whereas (*Z*)-$\mathbf{2^{CN}}$-**Mo** could be isolated cleanly by fractional crystallisation, the slow and partial isomerisation of (*Z*)-$\mathbf{2^{CN}}$-**W** to (*E*)-$\mathbf{2^{CN}}$-**W** in solution, even at room temperature, prevented the clean isolation of either isomer.

1 (*a*) P. L. Timms, *Acc. Chem. Res.*, 1973, **6**, 118; (*b*) P. L. Timms, *J. Am. Chem. Soc.*, 1967, **89**, 1629; (*c*) J. W. C. Johns, F. A. Grimm and R. F. Porter, *J. Mol. Spectrosc.*, 1967, **22**, 435.
2 (*a*) H. F. Bettinger, *J. Am. Chem. Soc.*, 2006, **128**, 2534; (*b*) C. A. Thompson, L. Andrews, J. M. L. Martin and J. El-Yazal, *J. Phys. Chem.*, 1995, **99**, 13839; (*c*) L. Andrews, P. Hassanzadeh, J. M. L. Martin and P. R. Taylor, *J. Phys. Chem.*, 1993, **97**, 5839.
3 Selected examples: (*a*) M. Ito, N. Tokitoh, T. Kawashima and R. Okazaki, *Tetrahedron Lett.*, 1999, **40**, 5557; (*b*) W. J. Grigsby and P. P. Power, *J. Am. Chem. Soc.*, 1996, **118**, 7981; (*c*) A. Meller, U. Seebold, W. Maringgele, M. Noltmeyer and G. M. Sheldrick, *J. Am. Chem. Soc.*, 1989, **111**, 8299; (*d*) B. Pachaly and R. West, *Angew. Chem., Int. Ed. Engl.*, 1984, **23**, 454.
4 Selected reviews: (*a*) H. Braunschweig, R. D. Dewhurst and V. H. Gessner, *Chem. Soc. Rev.*, 2013, **42**, 3197; (*b*) D. Vidovic, G. A. Pierce and S. Aldridge, *Chem. Commun.*, 2009, 1157; (*c*) H. Braunschweig, C. Kollann and F. Seeler,

Transition Metal Borylene Complexes, in *Contemporary Metal Boron Chemistry I. Structure and Bonding*, ed. T. B. Marder and Z. Lin, Springer, Berlin, Heidelberg, 2008, vol. 130.

5 (*a*) M.-A. Légaré, C. Pranckevicius and H. Braunschweig, *Chem. Rev.*, 2019, **119**, 8231; (*b*) M. Soleilhavoup and G. Bertrand, *Angew. Chem., Int. Ed.*, 2017, **56**, 10282.

6 R. Kinjo, B. Donnadieu, M. A. Celik, G. Frenking and G. Bertrand, *Science*, 2011, **333**, 610.

7 (*a*) U. S. D. Paul, M. J. Krahfuß and U. Radius, *Chem. Unserer Zeit*, 2018, **53**, 212; (*b*) M. Melaimi, R. Jazzar, M. Soleilhavoup and G. Bertrand, *Angew. Chem., Int. Ed.*, 2017, **56**, 10046; (*c*) M. Soleilhavoup and G. Bertrand, *Acc. Chem. Res.*, 2015, **48**, 256.

8 F. Dahcheh, D. Martin, D. W. Stephan and G. Bertrand, *Angew. Chem., Int. Ed.*, 2014, **53**, 13159.

9 (*a*) A. Hofmann, M.-A. Légaré, L. Wüst and H. Braunschweig, *Angew. Chem., Int. Ed.*, 2019, **58**, 9776; (*b*) M.-A. Légaré, G. Bélanger-Chabot, R. D. Dewhurst, E. Welz, I. Krummenacher, B. Engels and H. Braunschweig, *Science*, 2018, **359**, 896; (*c*) H. Braunschweig, I. Krummenacher, M.-A. Légaré, A. Matler, K. Radacki and Q. Ye, *J. Am. Chem. Soc.*, 2017, **139**, 1802.

10 (*a*) J. Böhnke, M. Arrowsmith and H. Braunschweig, *J. Am. Chem. Soc.*, 2018, **140**, 10368; (*b*) A. Stoy, J. Böhnke, J. O. C. Jimenéz-Halla, R. D. Dewhurst, T. Thiess and H. Braunschweig, *Angew. Chem., Int. Ed.*, 2018, **57**, 5947; (*c*) M. Arrowsmith, J. Böhnke, H. Braunschweig and M. A. Celik, *Angew. Chem., Int. Ed.*, 2017, **56**, 14287.

11 D. A. Ruiz, M. Melaimi and G. Bertrand, *Chem. Commun.*, 2014, **50**, 7837.

12 S. K. Sarkar, M. M. Siddiqui, S. Kundu, M. Ghosh, J. Kretsch, P. Stollberg, R. Herbst-Irmer, D. Stalke, A. C. Stückl, B. Schwederski, W. Kaim, S. Ghorai, E. D. Jemmis and H. W. Roesky, *Dalton Trans.*, 2019, **48**, 8551.

13 M. Arrowsmith, J. I. Schweizer, M. Heinz, M. Härterich, I. Krummenacher, M. C. Holthausen and H. Braunschweig, *Chem. Sci.*, 2019, **10**, 5095.

14 M. Arrowsmith, D. Auerhammer, R. Bertermann, H. Braunschweig, G. Bringmann, M. A. Celik, R. D. Dewhurst, M. Finze, M. Grüne, M. Hailmann, T. Hertle and I. Krummenacher, *Angew. Chem., Int. Ed.*, 2016, **55**, 14464.

15 S. Hagspiel, M. Arrowsmith, F. Fantuzzi, A. Vargas, A. Rempel, A. Hermann, T. Brückner and H. Braunschweig, *Angew. Chem., Int. Ed.*, 2021, **60**, 6446.

16 (*a*) L. Kong, R. Ganguly, Y. Li and R. Kinjo, *Chem. Sci.*, 2015, **6**, 2893; (*b*) L. Kong, Y. Li, R. Ganguly, D. Vidovic and R. Kinjo, *Angew. Chem., Int. Ed.*, 2014, **53**, 9280.

17 H. Braunschweig, R. D. Dewhurst, L. Pentecost, K. Radacki, A. Vargas and Q. Ye, *Angew. Chem., Int. Ed.*, 2016, **55**, 436.

18 H. Wang, L. Wu, Z. Lin and Z. Xie, *J. Am. Chem. Soc.*, 2017, **139**, 13680.

19 (*a*) M. Arrowsmith, J. Böhnke, H. Braunschweig, H. Gao, M.-A. Légaré, V. Paprocki and J. Seufert, *Chem.–Eur. J.*, 2017, **23**, 12210; (*b*) H. Braunschweig, R. D. Dewhurst, F. Hupp, M. Nutz, K. Radacki, C. W. Tate, A. Vargas and Q. Ye, *Nature*, 2015, **522**, 327; (*c*) D. P. Curran, A. Boussonnière, S. J. Geib and E. Lacôte, *Angew. Chem., Int. Ed.*, 2012, **51**, 1602; (*d*) Y. Wang and G. H. Robinson, *Inorg. Chem.*, 2011, **50**, 12326; (*e*) P. Bissinger, H. Braunschweig, A. Damme, R. D. Dewhurst, T. Kupfer, K. Radacki and K. Wagner, *J. Am. Chem. Soc.*, 2011, **133**, 19044.

20 (*a*) R. E. Bachman and K. H. Whitmire, *Inorg. Chem.*, 1995, **34**, 1542; (*b*) F. Biesemeier, K. Harms and U. Müller, *Z. Kristallogr.–New Cryst. Struct.*, 2014, **218**, 419; (*c*) J. Reibenspies, D. Darensbourg and E. Atnip, *Z. Kristallogr.–Cryst. Mater.*, 1994, **209**, 379.

21 A. Trummal, L. Lipping, I. Kaljurand, I. A. Koppel and J. Leito, *J. Phys. Chem. A*, 2016, **120**, 3663.

22 F. G. Bordwell and D. L. Hughes, *J. Org. Chem.*, 1982, **47**, 3224.

23 (*a*) S. Hagspiel, M. Arrowsmith, F. Fantuzzi, A. Hermann, V. Paprocki, R. Drescher, I. Krummenacher and H. Braunschweig, *Chem. Sci.*, 2020, **11**, 551; (*b*) D. Auerhammer, M. Arrowsmith, H. Braunschweig, R. D. Dewhurst, J. O. C. Jiménez-Halla and T. Kupfer, *Chem. Sci.*, 2017, **8**, 7066; (*c*) S. Wuertemberger-Pietsch, H. Schneider, U. Radius and T. B. Marder, *Chem.–Eur. J.*, 2016, **22**, 13032; (*d*) M. R. Momeni, E. Rivard and A. Brown, *Organometallics*, 2013, **32**, 6201.

24 A. K. Chandra, P.-C. Nam and M. T. Nguyen, *J. Phys. Chem. A*, 2003, **107**, 9182.

25 (*a*) E. P. L. Hunter and S. G. Lias, *J. Phys. Chem. Ref. Data*, 1998, **27**, 413; (*b*) M. P. Drapeau, A. Tlili, Y. Zaid, D. Toummini, F. O. Chahdi, J.-M. Sotiropoulos, T. Ollevier and M. Taillefer, *Chem.–Eur. J.*, 2018, **24**, 17449; (*c*) B. A. Trofimov, E. Y. Schmidt, I. A. Ushakov, N. V. Zorina, E. V. Skital'tseva, N. I. Protsuk and A. I. Mikhaleva, *Chem.–Eur. J.*, 2010, **16**, 8516.

26 R. Tonner, G. Heydenrych and G. Frenking, *ChemPhysChem*, 2008, **9**, 1474.